

# Th17 lymphocytes traffic to the central nervous system independently of $\alpha 4$ integrin expression during EAE

Veit Rothhammer, Sylvia Heink, Franziska Petermann, Rajneesh Srivastava, Malte C. Claussen, Bernhard Hemmer, and Thomas Korn

Klinikum rechts der Isar, Department of Neurology, Technical University Munich, 81675 Munich, Germany

**The integrin  $\alpha 4\beta 1$  (VLA-4) is used by encephalitogenic T cells to enter the central nervous system (CNS). However, both Th1 and Th17 cells are capable of inducing experimental autoimmune encephalomyelitis (EAE), and the molecular cues mediating the infiltration of Th1 versus Th17 cells into the CNS have not yet been defined. We investigated how blocking of  $\alpha 4$  integrins affected trafficking of Th1 and Th17 cells into the CNS during EAE. Although antibody-mediated inhibition of  $\alpha 4$  integrins prevented EAE when MOG<sub>35-55</sub>-specific Th1 cells were adoptively transferred, Th17 cells entered the brain, but not the spinal cord parenchyma, irrespective of  $\alpha 4$  blockade. Accordingly, T cell-conditional  $\alpha 4$ -deficient mice were not resistant to actively induced EAE but showed an ataxic syndrome with predominantly supraspinal infiltrates of IL-23R<sup>+</sup>CCR6<sup>+</sup>CD4<sup>+</sup> T cells. The entry of  $\alpha 4$ -deficient Th17 cells into the CNS was abolished by blockade of LFA-1 ( $\alpha L\beta 2$  integrin). Thus, Th1 cells preferentially infiltrate the spinal cord via an  $\alpha 4$  integrin-mediated mechanism, whereas the entry of Th17 cells into the brain parenchyma occurs in the absence of  $\alpha 4$  integrins but is dependent on the expression of  $\alpha L\beta 2$ . These observations have implications for the understanding of lesion localization, immunosurveillance, and drug design in multiple sclerosis.**

---

**CORRESPONDENCE**

Thomas Korn:  
korn@lrz.tum.de

Abbreviations used: CNS, central nervous system; EAE, experimental autoimmune encephalomyelitis; MS, multiple sclerosis.

VLA-4 is a heterodimeric integrin composed of  $\alpha 4$  and  $\beta 1$  subunits (Pribila et al., 2004). The monoclonal antibody natalizumab directed against  $\alpha 4$  was introduced into the treatment of multiple sclerosis (MS) because it had been recognized that encephalitogenic T cells used VLA-4 to infiltrate the central nervous system (CNS; Yednock et al., 1992; Baron et al., 1993; von Andrian and Engelhardt, 2003; Polman et al., 2006). Early studies in adoptive transfer experimental autoimmune encephalomyelitis (EAE) in mice suggested that only VLA-4-expressing CNS antigen-specific T cell lines were able to induce EAE, and blockade of VLA-4 by antibodies to  $\alpha 4$  abrogated their encephalitogenic potential (Baron et al., 1993; Kuchroo et al., 1993). Short-term T cell lines and encephalitogenic T cell clones are heavily biased toward production of IFN- $\gamma$  and fail to secrete IL-4 and IL-13 (Kuchroo et al., 1995). Hence, Th1 cytokine signature and VLA-4 expression co-segregate in encephalitogenic T cells. However, it is now clear that Th17 cells whose transcriptional program is essentially distinct from Th1 cells are also able to induce EAE

(Jäger et al., 2009; Domingues et al., 2010). Th17 cells even appear superior to Th1 cells in their strength to induce tissue inflammation in solid organs and thus have recently been associated with a variety of autoimmune diseases including psoriasis, rheumatoid arthritis, and MS (Murphy et al., 2003; Langrish et al., 2005; Hirota et al., 2007; Zheng et al., 2007; Lowes et al., 2008; Durelli et al., 2009; Kebir et al., 2009). Th17 cells express the IL-23 receptor (IL-23R), and the exquisite pathogenicity of Th17 cells may be associated with their capacity to respond to IL-23 (Mangan et al., 2006; Manel et al., 2008; Awasthi et al., 2009; McGeachy et al., 2009).

Although it has been suggested in a recent study that the chemokine receptor CCR6 guides the entry of Th17 cells into the CNS through the ependymal layer (Reboldi et al., 2009), it has not yet been directly addressed whether Th1

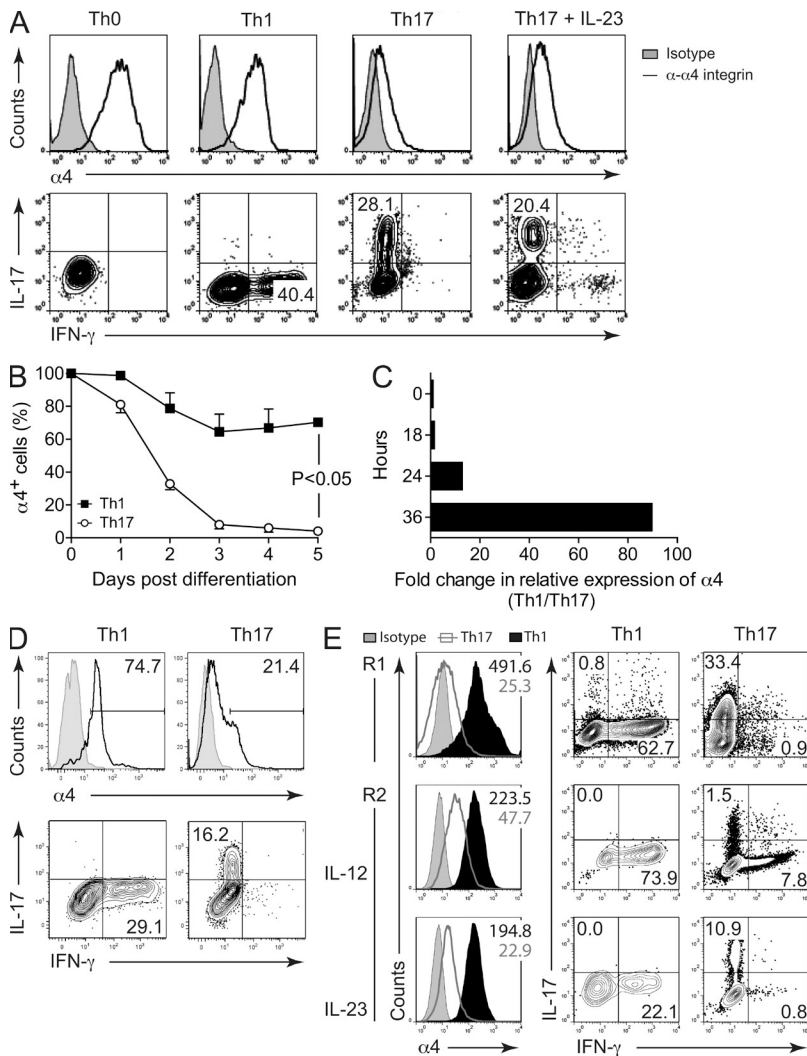


**Figure 1. Expression of  $\alpha 4$  integrin mRNA and protein are down-regulated in Th17 cells.** (A) Purified naive T cells ( $CD4^+CD44^-Foxp3^-$ ) isolated from *Foxp3gfp.KI* mice were cultured under Th0 (no cytokines), Th1 (IL-12 and anti-IL-4), or Th17 (TGF- $\beta$  plus IL-6  $\pm$  IL-23) polarizing conditions with polyclonal TCR stimulation. On day 3, expression of  $\alpha 4$  integrin was determined by surface staining (top row: tinted line, isotype control; black line,  $\alpha 4$ -integrin). The differentiation status was confirmed by intracellular cytokine staining (bottom row: numbers indicate percentages of cytokine-positive cells). Shown are representatives of more than five independent experiments. (B) Time course of  $\alpha 4$  integrin expression during Th1 and Th17 differentiation as determined by surface staining (means  $\pm$  SD,  $n = 4$ , Student's *t* test). (C) RNA was isolated from T cells that had been stimulated under Th1 or Th17 polarizing conditions at indicated time points. Relative expression of  $\alpha 4$  integrin was determined by quantitative RT-PCR analysis. Bars indicate fold change in relative expression of  $\alpha 4$  integrin in Th1 versus Th17 cells. Shown are representatives of four independent experiments. (D) Naive T cells ( $CD4^+CD44^-Foxp3^-$ ) from 2D2  $\times$  *Foxp3gfp.KI* MOG<sub>35-55</sub>-specific TCR transgenic mice were cultivated 1:5 with irradiated syngeneic splenocytes as APCs and 20  $\mu$ g/ml MOG<sub>35-55</sub> peptide under Th1 or Th17 polarizing conditions, respectively.  $\alpha 4$  integrin expression and cytokine status were determined on day 4 after the start of differentiation by flow cytometry. Shown are representatives of two independent experiments. (E) Naive ( $CD4^+CD44^-CD25^-$ ) T cells were FACS sorted and polarized under Th1 or Th17 conditions (R1). After a resting phase, T cells were restimulated by plate-bound anti-CD3 and soluble anti-CD28 antibodies in the presence of IL-12 or IL-23 (R2) and allowed to proliferate for another 3 d before analyzing the expression levels of surface  $\alpha 4$  integrin and intracellular IL-17 and IFN- $\gamma$  by flow cytometry (numbers indicate percentages of cytokine-positive cells). In the histogram plots, numbers indicate mean fluorescence intensity (MFI) of  $\alpha 4$  integrin surface expression in Th1 (black numbers) or Th17 cells (gray numbers), respectively. Shown are representatives of two independent experiments.

and Th17 cells use different entry routes into the CNS. Even though it has been suggested that Th17 cells might rely on other integrins as compared with Th1 cells when crossing the blood/cerebrospinal fluid barrier or the blood-brain barrier (Wang et al., 2007; Kebir et al., 2009), the use of particular integrins by Th1 cells versus Th17 cells has not yet been correlated with the accumulation of encephalitogenic T cell subsets in topographically distinct niches of the CNS. In the present study, we investigated the requirement for  $\alpha 4$  integrins, particularly VLA-4 ( $\alpha 4\beta 1$ , CD49d/CD29), and also the  $\beta 2$  integrin LFA-1 ( $\alpha L\beta 2$ , CD11a/CD18) in the entry of T cell subsets into the CNS. We observed that  $\alpha 4$  integrin is down-regulated in the Th17 expression profile, whereas antigen-specific Th1 cells expressed high amounts of  $\alpha 4$  integrin. Accordingly, Th1 cell-mediated EAE, but not Th17 cell-mediated EAE, was blocked by a monoclonal antibody to  $\alpha 4$  integrin. Under  $\alpha 4$  blockade, recipients of encephalitogenic Th17 cells developed atypical EAE with ataxic hemiparesis, a clinical phenotype which was recapitulated in actively induced EAE of T cell conditional  $\alpha 4$ -deficient mice. Blockade of LFA-1 completely

abolished the disease in T cell conditional  $\alpha 4$  integrin-deficient mice but resulted in severe EAE in wild-type animals. We conclude that expression of  $\alpha 4$  integrin is necessary and sufficient for myelin antigen-specific Th1 cells to enter the CNS. However, Th17 cells are able to use  $\beta 2$  integrins to infiltrate into the CNS and are able to enter the target tissue independently of  $\alpha 4$  integrin expression.

## RESULTS

Th17 cells express lower amounts of  $\alpha 4$  integrin than Th1 cells

Both Th1 and Th17 cells are capable of inducing EAE. We were interested in evaluating whether Th1 and Th17 cells used different integrins to enter the CNS compartment. Because heterodimeric  $\alpha 4\beta 1$  (VLA-4) has been identified to be essential for encephalitogenic T cells to invade the CNS (Baron et al., 1993), we first tested the expression profile of  $\alpha 4$  integrin in Th1 and Th17 cells. Naive T cells ( $CD4^+CD44^-Foxp3^-$ ) were purified from the peripheral immune compartment of *Foxp3gfp* knockin (*Foxp3gfp.KI*) mice and differentiated into Th1 or Th17 cells *in vitro* (Fig. 1 A). On day 4 after start of differentiation,

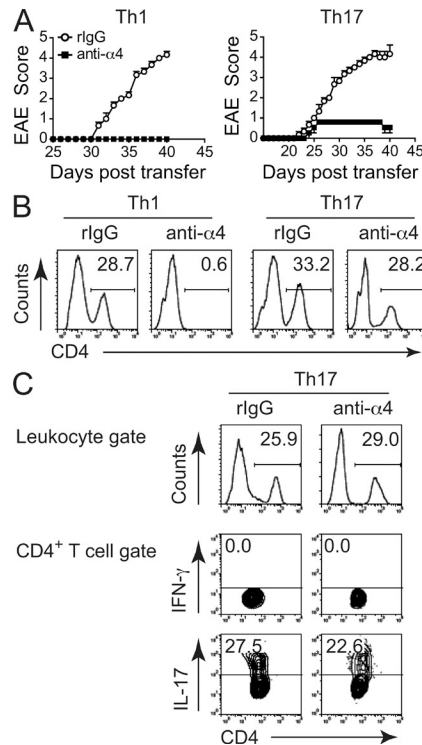


**Figure 2. In adoptive transfer EAE, antigen-specific Th17, but not Th1, cells enter into CNS independently of  $\alpha 4$  blockade.** (A) Naive CD4 $^{+}$ CD44 $^{-}$ CD25 $^{-}$  T cells from 2D2 MOG<sub>35-55</sub>-specific TCR transgenic mice were polarized under Th1 or Th17 conditions in vitro. On day 3, cytokine status was checked by intracellular cytokine staining and  $2 \times 10^6$  cytokine-positive cells were injected i.v. into  $Rag1^{-/-}$  mice. Before injection, polarized cells were incubated with control Ig or blocking antibodies to  $\alpha 4$  integrin (PS/2). According to the pretreatment of the transferred cells, host mice were administered rlgG or anti- $\alpha 4$  antibody every 3 d until the development of disease. Means of clinical scores  $\pm$  SEM,  $n = 4$ . Note that host mice that received Th17 cells under conditions of  $\alpha 4$  blockade developed signs of atypical EAE with ataxia and hemiparesis. (B) At the peak of disease, mononuclear cells were isolated from the CNS of individual mice, stained for CD3 and CD4, and analyzed by flow cytometry. Numbers in the histograms represent percentages of CD4 $^{+}$  T cells among CNS-infiltrating mononuclear cells. Shown are representatives of six independent experiments. (C) MOG<sub>35-55</sub>-specific TCR transgenic 2D2 mice were crossed to  $Ifng^{-/-}$  mice. Naive T cells were differentiated under Th17 conditions and transferred into  $Rag1^{-/-}$  mice, which were then treated with rlgG or blocking antibodies to  $\alpha 4$  integrin. CNS-infiltrating mononuclear cells were isolated at the peak of disease and stained for surface and intracellular antigens as indicated. Shown are representatives of three independent experiments.

cytokine expression profile and expression of  $\alpha 4$  integrin (CD49d) were determined by flow cytometry and quantitative RT-PCR (Fig. 1, A–C). Under Th1 differentiation conditions, T cells expressed IFN- $\gamma$  and high amounts of  $\alpha 4$  integrin throughout the differentiation culture. In contrast, differentiation of naive T cells into the Th17 phenotype was associated with a significant decrease in  $\alpha 4$  integrin expression both on the protein and mRNA levels irrespective of whether or not IL-23 was present during T cell differentiation (Fig. 1, A and B). The decrease of  $\alpha 4$  integrin expression under Th17, but not Th1,

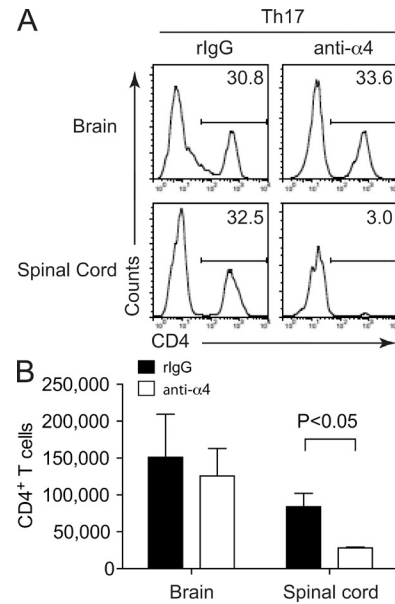
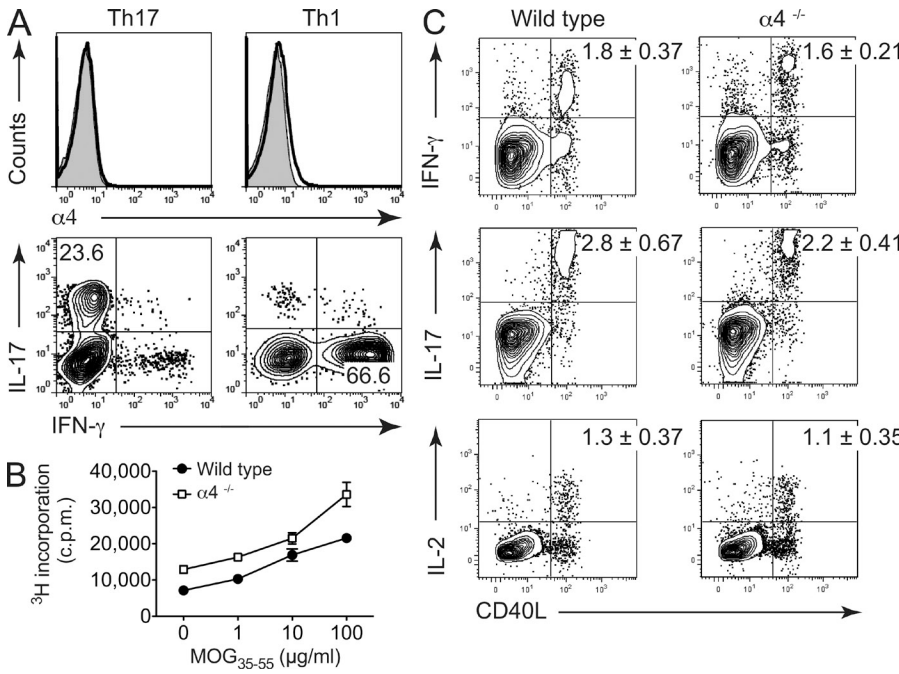


**Figure 3. Encephalitogenic Th17 cells enter supraspinal parts of the CNS but fail to migrate into the spinal cord when  $\alpha 4$  integrins are blocked.** (A) Naive T cells from 2D2 mice were differentiated into Th17 cells in vitro and transferred into  $Rag1^{-/-}$  mice, which were treated with control rlgG or blocking antibodies to  $\alpha 4$  integrin (see Fig. 2). At the peak of disease, the CNS was prepared and dissected into brain (brain stem, cerebellum, and cerebrum) and spinal cord. Mononuclear cells were isolated separately and analyzed by flow cytometry. Numbers indicate percentages of CD3 $^{+}$ CD4 $^{+}$  T cells within the live mononuclear cell compartment. Shown are representatives of five independent experiments. (B) Quantification of absolute numbers of CD3 $^{+}$ CD4 $^{+}$  T cells infiltrating brain or spinal cord under treatment with control rlgG or antibodies to  $\alpha 4$  (mean  $\pm$  SD,  $n = 4$ ).

differentiation conditions was equally observed when purified naive MOG<sub>35-55</sub>-specific TCR transgenic T cells (2D2) were stimulated with their cognate antigen in the presence of antigen-presenting cells (Fig. 1 D). When Th17 cells were removed from the differentiation culture and rested,  $\alpha 4$  integrin was reexpressed to some extent although Th1 levels were never reached. Upon round two of restimulation in the presence of IL-23, committed Th17 cells kept down-regulating the expression of  $\alpha 4$  again. In contrast, Th1 cells showed elevated amounts of  $\alpha 4$  integrin throughout the primary and secondary cultures (Fig. 1 E). Thus, decreased levels of  $\alpha 4$  expression appear to be associated with the Th17 but not the Th1 developmental pathway.

#### Entry of Th1 but not Th17 cells into CNS is blocked by antibodies to $\alpha 4$ integrin in adoptive transfer EAE

To determine the functional relevance of the down-regulation of  $\alpha 4$  in Th17 cells in an EAE model, naive CD4 $^{+}$ CD44 $^{-}$ CD25 $^{-}$  T cells from 2D2 mice were FACS sorted and differentiated into Th1 or Th17 cells in vitro, followed by transfer into  $Rag1^{-/-}$  recipient mice.  $2 \times 10^6$  IFN- $\gamma$  or IL-17 single producers were transferred, respectively. Before transfer, Th1 and Th17 cells were incubated with control immunoglobulin or blocking antibodies to  $\alpha 4$  integrin (PS/2) and after transfer, host mice



were treated with either control IgG or antibodies to α4 integrin until the development of first signs of disease. In the absence of α4 blockade, both Th1 and Th17 cells induced classical EAE with ascending paralysis (Fig. 2 A). In contrast, treatment with anti-α4 antibodies completely abrogated the development of signs of disease when Th1 cells were transferred (Fig. 2 A, left). However, blockade of α4 integrins failed to abolish EAE upon transfer of Th17 cells (Fig. 2 A, right). Consistent with the clinical outcome, infiltration of the CNS with CD4<sup>+</sup> T cells was eliminated by anti-α4 treatment in Th1 cell-transferred animals but not in mice that received Th17 cells (Fig. 2 B). The cytokine phenotype of Th17 cells was unstable and a significant fraction of previously pure IL-17 producers expressed IFN-γ after transfer into host mice (Kurschus et al., 2010; not depicted). Hence, we wanted to test whether re-expression of IFN-γ was associated with the resistance to α4 blockade in Th17 cells. We crossed 2D2 mice into the IFN-γ KO background and differentiated naive T cells from these mice into Th17 cells followed by transfer into Rag1-deficient mice without or with blockade of α4 integrin. Here, Th17 cells remained stable IL-17 producers after transfer. However, similar to what we observed with regular 2D2 T cells, α4 blockade was not able to abrogate the entry of IFN-γ-deficient Th17 cells into the CNS (Fig. 2 C), suggesting that the initial commitment of T cells to the Th17 developmental program was sufficient to render their encephalitogenic potential resistant to α4 blockade.

Mice transferred with Th17 cells developed atypical EAE under anti-α4 treatment. The animals showed severe gait ataxia or hemiparesis, signs of cerebral rather than spinal cord disease (Video 1). Therefore, we dissected the spinal cord from the cerebrum and purified infiltrating mononuclear cells separately. Under α4 blockade, Th17 cells were prevented from entering the spinal cord but not the cerebrum, suggesting an

**Figure 4.** T cell differentiation and antigen-specific proliferation is not impaired in *CD4 Cre × α4<sup>fl/fl</sup>* mice. We generated T cell conditional α4 integrin knockout mice (α4<sup>-/-</sup>) by crossing *CD4 Cre* mice with *α4<sup>fl/fl</sup>* mice.

(A) Naive T cells (CD4<sup>+</sup>CD44<sup>-</sup>CD25<sup>-</sup>) from α4<sup>-/-</sup> mice were isolated by FACS sorting and differentiated in vitro by stimulation with anti-CD3/anti-CD28 under Th1 or Th17 polarizing conditions. Surface staining for α4 integrin (top row: tinted line, isotype control; black line, anti-α4 integrin) and intracellular cytokine staining for IL-17 and IFN-γ (bottom row) are depicted. Numbers indicate percentages of cytokine-positive cells. Shown are representatives of three independent experiments. (B and C) α4<sup>-/-</sup> mice and wild-type littermates were immunized with MOG<sub>35-55</sub> in CFA. On day 8, draining lymph nodes were dissected and restimulated with MOG<sub>35-55</sub> in vitro. After 48 h, the antigen-specific proliferative response was determined by <sup>3</sup>H-thymidine incorporation (B, means + SD,  $n = 3$ ). (C) Fractions of antigen-specific cytokine-producing CD4<sup>+</sup> T cells in draining lymph nodes of MOG<sub>35-55</sub>-immunized wild-type and conditional α4<sup>-/-</sup> mice were determined by intracellular CD40L (CD154) and cytokine staining after restimulation with MOG<sub>35-55</sub>. Numbers indicate percentages of cytokine/CD40L double-positive cells (C, means ± SEM,  $n = 3$ ).

α4-dependent entry mechanism into the spinal cord but not into the cerebrum (Fig. 3, A and B).

#### Conditional knockout of α4 integrin in CD4<sup>+</sup> T cells causes atypical EAE as a result of predominant cerebral infiltration

As experimental approaches using blocking antibodies may lead to an incomplete inhibition of α4 integrins, we crossed *α4<sup>fl/fl</sup>* mice with *CD4 Cre* mice to generate conditional α4 integrin-deficient animals, in which all T cells would lack α4 integrin (α4<sup>-/-</sup> mice). As expected, CD4<sup>+</sup> T cells did not express α4 integrin but displayed full differentiation capacity into Th1 and Th17 cells upon polyclonal stimulation in vitro (Fig. 4 A). It has been reported that engagement of VLA-4 within the immunological synapse might impair the development of Th2 cells (Mittelbrunn et al., 2004). Thus, we

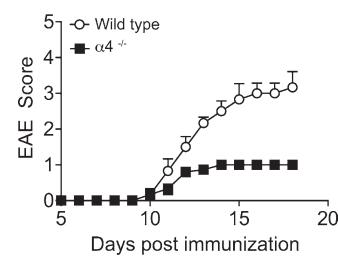


**Figure 5.** α4<sup>-/-</sup> mice develop atypical EAE. EAE was induced in α4<sup>-/-</sup> mice or wild-type control animals by immunization with MOG<sub>35-55</sub> in CFA and disease severity was monitored according to the classical EAE score (mean clinical score + SEM,  $n = 5$ ). Note that α4<sup>-/-</sup> mice developed an ataxic EAE syndrome whose severity is only partially reflected in the classical EAE score.

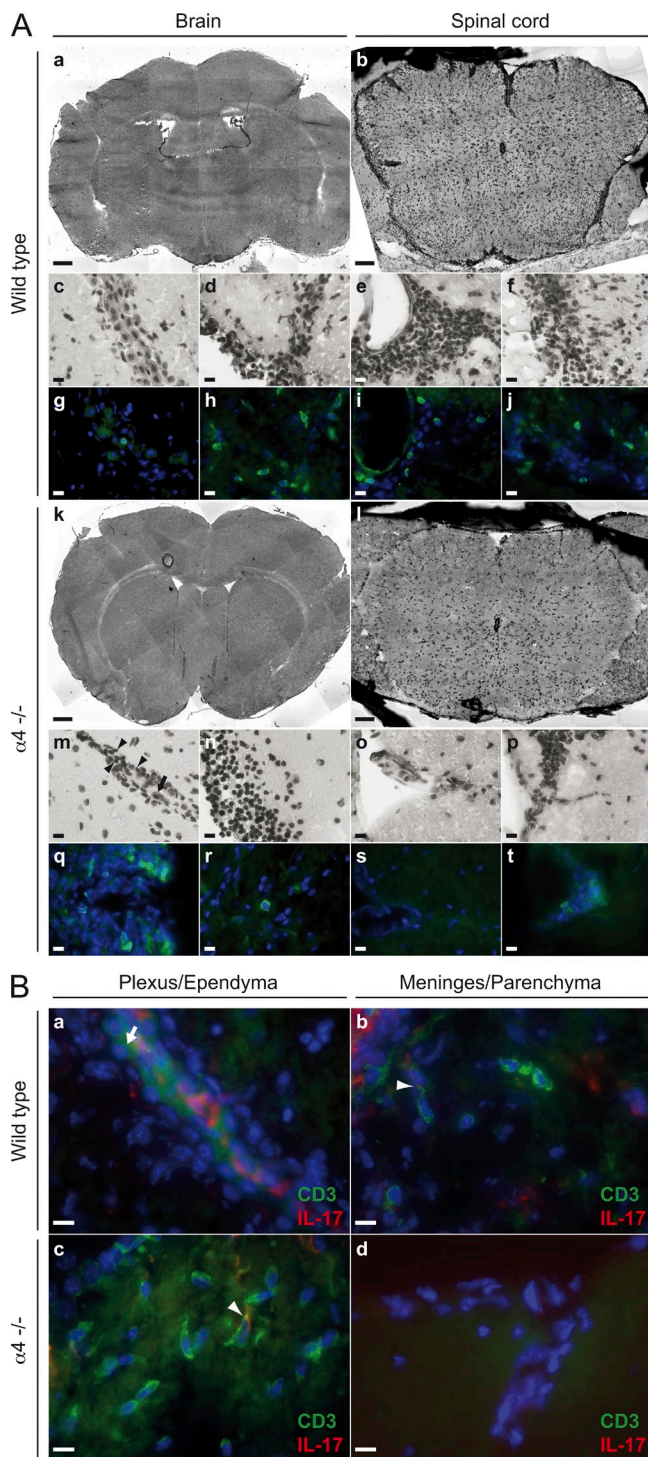


**Figure 6.  $\alpha 4^{-/-}$  mice develop atypical EAE as a result of predominant cerebral immune cell infiltration.** At the peak of disease (i.e., on day 18 after immunization), coronal brain sections and transverse lumbar spinal cord sections were prepared from MOG<sub>35-55</sub>-immunized wild-type and  $\alpha 4^{-/-}$  mice. (A) Light microscopy of sections stained with hematoxylin and eosin (a-f and k-p) and immunofluorescence imaging of sections stained for CD3 (green, g-j and q-t). Note that there were hardly any CD3<sup>+</sup> T cells in the plexus epithelium of wild-type mice (c and g), whereas inflammatory infiltrates were identified beneath the glia limitans (d and h). In contrast,  $\alpha 4^{-/-}$

tested the in vivo sensitization against MOG<sub>35-55</sub> in  $\alpha 4^{-/-}$  mice in a quantitative and qualitative manner. After active immunization with MOG<sub>35-55</sub>, CD4<sup>+</sup> T cells from draining lymph nodes of T cell conditional  $\alpha 4$ -deficient animals showed high MOG<sub>35-55</sub>-specific recall responses that were similar to recall responses in wild-type mice (Fig. 4 B). Also, the amounts of IFN- $\gamma$  and IL-17 that were produced by MOG<sub>35-55</sub>-activated CD4<sup>+</sup>CD40L<sup>+</sup> T cells from draining lymph nodes were equivalent in wild-type and  $\alpha 4^{-/-}$  mice (Fig. 4 C). These data suggested that antigen-specific sensitization with MOG<sub>35-55</sub> in CFA was not impaired under conditions of T cell-restricted absence of  $\alpha 4$  integrin.

As compared with their wild-type littermates, which developed classical EAE,  $\alpha 4^{-/-}$  mice immunized with MOG<sub>35-55</sub> in CFA mainly developed atypical disease with hemiparesis or ataxic gait (Fig. 5). When analyzing the sites of immunopathological damage within the CNS, we found that cellular infiltrates in  $\alpha 4^{-/-}$  mice were localized in the brain stem, cerebellum, and cerebrum, whereas the load of immune cell infiltration in the spinal cord was markedly reduced as compared with wild-type littermates (Fig. 6 A). T cell recruitment around meningeal vessels and perivascular T cell accumulation within the CNS parenchyma was prominent in wild-type mice, suggesting a vascular recruitment pattern in the CNS and especially in the spinal cord of wild-type mice (Fig. 6 A). In contrast,  $\alpha 4^{-/-}$  mice showed marked immune cell infiltrates within the plexus epithelium or in the brain parenchyma adjacent to the cerebral ventricles (Fig. 6 A). Parenchymal T cell infiltrates in the spinal cord were markedly reduced in  $\alpha 4^{-/-}$  mice as compared with their wild-type counterparts (Fig. 6 A). Colocalization of IL-17 with T cells was most clearly observed in the ventricle-associated areas of  $\alpha 4^{-/-}$  mice (Fig. 6 B). Together, these data indicated that encephalitogenic T cells might be redirected to cerebrospinal fluid-associated anatomical niches in the absence of  $\alpha 4$  integrin expression. We then determined the number and functional phenotype of CD4<sup>+</sup> T cells recovered from the brain and spinal cord in a quantitative manner by flow cytometry. Here, we observed that the absolute numbers of CD4<sup>+</sup> T cells at the peak of disease were significantly lower in the spinal cord (but not the brain) of  $\alpha 4^{-/-}$  mice as compared with wild-type littermates (Fig. 7, A and B). The cytokine profile of T cells (IL-17, IFN- $\gamma$ , and IL-17/IFN- $\gamma$  double-positive CD4<sup>+</sup> T cells) infiltrating the cerebrum was comparable between wild-type and  $\alpha 4^{-/-}$  mice. However, in the spinal cord of  $\alpha 4^{-/-}$  mice, there was a significant reduction in the number of

animals showed T cells associated with the plexus epithelium (m and q) as well as the meninges (n and r). The arrowheads in m indicate inflammatory cells associated with ventricular epithelium lining. The arrow in m designates a ventricular epithelial lining cell. (B) Double immunofluorescence staining for CD3 (green) and IL-17 (red) in cryosections from wild-type (a and b) and  $\alpha 4^{-/-}$  EAE mice (c and d). Nuclear staining with DAPI is shown (blue). IL-17-producing T cells (yellow, arrowheads in b and c) were identified in meningeal infiltrates of wild-type mice (b) and in the periventricular infiltrates of  $\alpha 4^{-/-}$  animals (c). The arrow in a indicates a plexus epithelial cell. Bars: (A, a and k) 500  $\mu$ m; (A, b and l) 125  $\mu$ m; (A, c-j and m-t; B, a-d) 10  $\mu$ m.

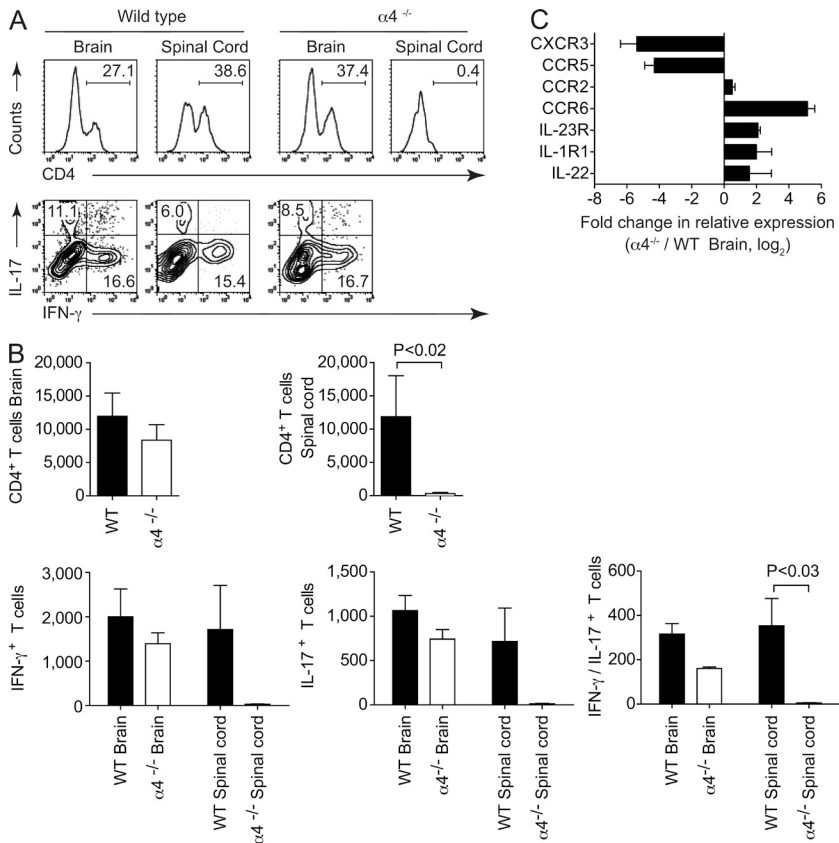


**Figure 7. Flow cytometric analysis of CNS-infiltrating T cells in MOG<sub>35-55</sub>-immunized wild-type versus α4<sup>-/-</sup> mice at the peak of EAE.**

Wild-type and α4<sup>-/-</sup> mice were immunized with MOG<sub>35-55</sub> plus CFA and, at the peak of disease, cerebrum and spinal cord were analyzed separately.

(A) Fraction and cytokine profile of CNS-infiltrating CD3+CD4+ T cells. Numbers indicate percentages of CD4<sup>-/-</sup> T cells among live mononuclear cells (top row) or percentages of cytokine-positive cells within the CD3+CD4+ T cell compartment (bottom row, representative of five independent experiments). (B) Absolute number of CD4+ T cells within the brain (top row, left) or spinal cord (top row, right) of wild-type or α4<sup>-/-</sup> EAE mice. In the bottom row, absolute numbers of IFN-γ, IL-17, or IFN-γ/IL-17 double-positive CD4+ T cells recovered from the brain or spinal cord of wild-type versus α4<sup>-/-</sup> mice are depicted (means + SD, n = 5). (C) CD3+CD4+ T cells were highly purified by FACS sorting from supraspinal parts of the CNS (brain, i.e. brain stem, cerebellum, and cerebrum) of MOG<sub>35-55</sub>-immunized wild-type or α4<sup>-/-</sup> mice at the peak of disease. Fold change in relative abundance of Cxcr3, Ccr5, Ccr2, Ccr6, Il23r, Il1r1, and Il-22 mRNA in α4<sup>-/-</sup> versus wild-type control mice (log scale, means + SD, n = 3).

cytokine-producing CD4<sup>+</sup> T cells irrespective of their commitment to IFN-γ or IL-17 production (Fig. 7, A and B).

To further investigate the actual lineage commitment of T cells infiltrating the cerebrum of wild-type versus α4<sup>-/-</sup> animals, brain-infiltrating CD3+CD4+ T cells from wild-type and α4<sup>-/-</sup> mice were FACS sorted at the peak of disease and analyzed as to their gene expression profile by quantitative PCR analysis. Notably, CD3+CD4+ effector T cells purified from the brain of α4<sup>-/-</sup> mice expressed markedly lower amounts of CXCR3 and CCR5 but higher amounts of CCR2, CCR6, IL-1R, and IL-23R as compared with their wild-type counterparts (Fig. 7 C), suggesting that α4<sup>-/-</sup> T cells infiltrating the brain were previously committed to the Th17 lineage in spite of their loss in actual production of IL-17A (Hirota et al., 2011). From these data, we concluded that commitment to the Th17 lineage in the peripheral immune compartment licenses T cells to enter the CNS, and here particularly the supraspinal parts of the CNS, in the absence of α4 integrin expression.

To directly compare the capacity of highly pure MOG<sub>35-55</sub>-specific Th17 versus Th1 cells to traffic into the CNS in the absence of α4 integrin expression, we crossed α4<sup>-/-</sup> mice onto the 2D2 background. Thus, we were able to isolate naïve (CD4+CD44-CD25-) MOG<sub>35-55</sub> TCR transgenic T cells that genetically lacked α4 expression. α4-deficient 2D2 T cells were differentiated into either Th1 or Th17 cells followed by adoptive transfer into Rag1-deficient host mice (Fig. 8). Although α4<sup>-/-</sup> Th1 2D2 cells failed to induce any signs of EAE, as

host mice that had received α4-deficient Th17 2D2 cells developed an ataxic EAE syndrome (Fig. 8, A and B). α4<sup>-/-</sup> Th1 and Th17 2D2 cells were equally suited to re-

locate to the peripheral immune tissue (Fig. 8 C). However, α4<sup>-/-</sup> Th1 2D2 cells were blocked from entering the CNS compartment. In contrast, α4<sup>-/-</sup> Th17 2D2 cells were not blocked from trafficking into the CNS and again infiltrated preferentially into supraspinal areas of the CNS (Fig. 8 C). These data corroborate that α4 expression is required for Th1 cells, but not for Th17 cells, to access the CNS parenchyma and initiate inflammatory lesions, although we cannot formally exclude that Th1 cells might also use other integrins in addition to VLA-4, particularly under conditions of increased tissue susceptibility to inflammation like in IFN-γ receptor-deficient mice or under conditions of ongoing inflammation.

#### Atypical EAE as a result of cerebral infiltration of α4 integrin-deficient T cells is inhibited by anti-CD11a treatment

Because myelin antigen-specific Th17 cells are able to traffic into the CNS parenchyma in the absence of α4 integrin expression, we wanted to define potential integrin candidates that are used by Th17 cells instead of VLA-4. We focused on β2 integrins because their role in the entry of encephalitogenic T cells has been confirmed previously (Archelos et al., 1993). CD4+ T cells infiltrating the brains of both wild-type and α4<sup>-/-</sup> mice expressed high amounts of integrin αL (CD11a) that combines with β2 to form LFA-1 (Fig. 9 A), making CD11a a possible candidate for an alternative adhesion molecule in the absence of integrin α4. In contrast to α4 integrin expression, which was reduced in Th17 cells as

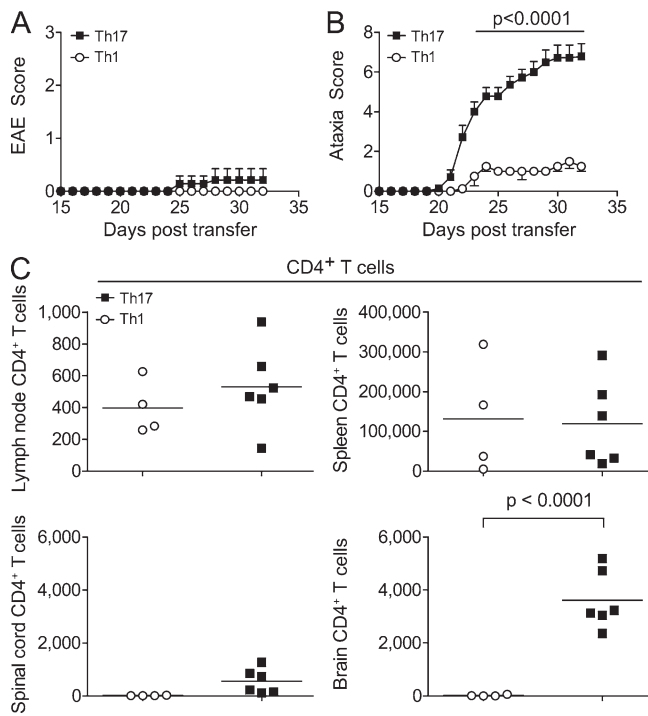


**Figure 8. Adoptive transfer of  $\alpha 4$ -deficient MOG<sub>35-55</sub>-specific TCR transgenic T cells (2D2) into *Rag1*<sup>-/-</sup> mice after in vitro polarization into Th1 or Th17 cells.** Naive T cells from 2D2  $\times$  CD4 Cre  $\times$   $\alpha 4$ <sup>fl/fl</sup> mice ( $\alpha 4$ <sup>-/-</sup> 2D2) were differentiated into Th1 or Th17 cells in vitro and transferred into *Rag1*<sup>-/-</sup> recipient mice. The host mice were followed clinically according to the classical EAE score (A) and according to an ataxia score (B). Means of clinical scores + SEM for classical and ataxic EAE are depicted (two-way ANOVA plus Bonferroni's post-testing). (C) At the peak of disease, lymph nodes, spleens, spinal cords, and brains (i.e. brain stem, cerebellum, and cerebrum) were dissected. Mononuclear cells were isolated separately and analyzed by flow cytometry. Quantification of absolute numbers of  $\alpha 4$ -deficient 2D2 CD3<sup>+</sup>CD4<sup>+</sup> T cells in lymph nodes and spleen (C, top row) and in spinal cord and brain (C, bottom row) reisolated from individual host mice (Student's *t* test). Horizontal bars indicate mean.

compared with their Th1 counterparts, in vitro differentiation of both Th1 and Th17 cells resulted in high amounts of CD11a expression (Fig. 9 B). We hypothesized that T cells that lack  $\alpha 4$  expression used LFA-1 to enter into the CNS parenchyma. To test this hypothesis, EAE was induced in wild-type and conditional  $\alpha 4$ <sup>-/-</sup> mice, which were subsequently treated with i.p. injections of anti-CD11a or isotype control antibodies starting on day 5 after immunization to avoid an impairment of T cell priming (Fig. 9, C and D). In the wild-type group, both isotype and anti-CD11a-treated animals developed severe classical EAE (Fig. 9 C). If anything, MOG<sub>35-55</sub>-induced EAE in wild-type mice seemed to be enhanced by treatment with anti-CD11a antibodies, supporting the idea that sensitization of encephalitogenic T cells in the peripheral immune compartment was not reduced upon administration of anti-CD11a antibodies according to our treatment regimen. In contrast, in conditional  $\alpha 4$ <sup>-/-</sup> animals, atypical EAE was entirely abolished as long as the animals were treated with anti-CD11a (Fig. 9, C and D). This clinical

observation was further corroborated when we analyzed the amount of CD4<sup>+</sup> T cells infiltrating the brain and spinal cord of the various experimental groups. Whereas wild-type animals displayed elevated CD4<sup>+</sup> T cell numbers in the brain under CD11a blockade, the infiltration of  $\alpha 4$ <sup>-/-</sup> T cells was efficiently inhibited by anti-CD11a treatment (Fig. 9, E and F). Collectively, these data support the idea that under conditions of  $\alpha 4$  deficiency, infiltration of antigen-specific T cells into the brain parenchyma is mediated by  $\alpha L$  integrin (CD11a), which may as well be the preferential adhesion molecule used by Th17 cells invading the supraspinal parts of the CNS.

## DISCUSSION

In the present study, we investigated the relative importance of  $\alpha 4$  integrin expression for the migration of distinct effector T cell subsets into the CNS during EAE. The key conclusions from our genetic and antibody-blocking approaches are that encephalitogenic T cells use both  $\alpha 4\beta 1$  and  $\alpha L\beta 2$  integrins to infiltrate into the CNS, that Th1 cells are dependent on  $\alpha 4$  integrin expression to enter into the CNS, and that Th17 cells are able to infiltrate into supraspinal parts of the CNS in the absence of  $\alpha 4$  integrin expression but in an LFA-1-dependent manner.

T cell-associated integrins are required for the firm adhesion and diapedesis of encephalitogenic T cells at the luminal membrane of CNS endothelial cells and at the abluminal membrane of ependymal cells. Both  $\alpha 4\beta 1$  (VLA-4) and  $\alpha L\beta 2$  (LFA-1) have been implicated in this process (Vajkoczy et al., 2001; Laschinger et al., 2002; Engelhardt and Sorokin, 2009). VLA-4 interacts with molecules of the extracellular matrix like the fibronectin fragment CS-1, but also with VCAM-1 on endothelial cells, and mediates firm adhesion of T cells while LFA-1 interacts with ICAM-1 or ICAM-2. ICAM-1 participates in attaching T cells to the endothelial surface, and both ICAM-1 and ICAM-2 are required for T cells to polarize followed by ICAM-1-dependent crawling against the blood stream under conditions of shear (Steiner et al., 2010). These sequential phases (adhesion, crawling, and diapedesis) have been documented in vitro and in vivo using experimental systems that were based on terminally committed IFN- $\gamma$ -producing encephalitogenic Th1 cells (Bartholomäus et al., 2009). However, both Th1 and Th17 cells contribute to the induction of inflammation in EAE (Langrish et al., 2005; Korn et al., 2007; Jäger et al., 2009; Domingues et al., 2010), and it has been proposed that Th1 cells and Th17 cells differ in their addressin equipment in vitro and in vivo (Langrish et al., 2005; Gyülvészi et al., 2009; Kebir et al., 2009).

The amount of  $\alpha 4$  integrin expression was significantly lower in MOG-specific Th17 cells than in their Th1 counterparts. Accordingly, EAE was completely inhibited by blockade of  $\alpha 4$  in Th1 transfer EAE but not in EAE adoptively transferred by Th17 cells. When integrin molecules are only available in low concentrations, integrin function is determined by avidity, the product of affinity and local clustering of the integrin (lateral mobility), which may be more easily blocked by anti- $\alpha 4$  antibodies than high-affinity binding of the integrin to its ligand alone which is exclusively relevant under conditions of high integrin expression. Antibody-mediated blockade of  $\alpha 4$

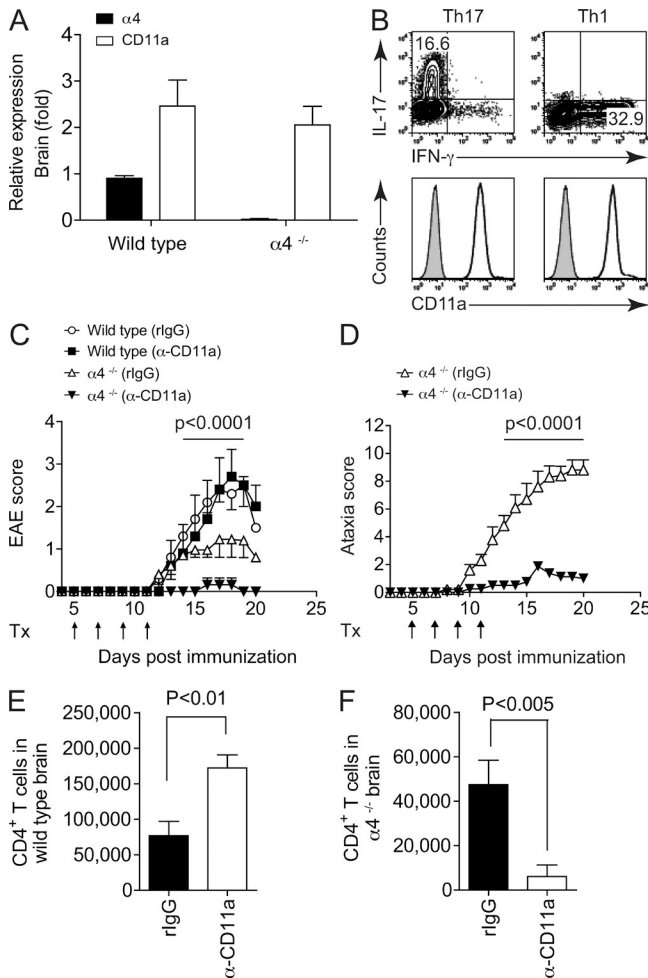


**Figure 9. Atypical EAE in  $\alpha 4^{-/-}$  mice and predominant cerebral T cell infiltration are inhibited by administration of blocking antibodies to CD11a (αL integrin).** EAE was induced in wild-type and T cell conditional  $\alpha 4^{-/-}$  mice by immunization with MOG<sub>35–55</sub> plus CFA. (A) Relative expression of  $\alpha 4$  integrin and CD11a (αL integrin) in CD4 $^{+}$  T cells isolated from the brain of untreated wild-type or  $\alpha 4^{-/-}$  EAE mice (means  $\pm$  SD,  $n = 3$ ). (B) Naive wild-type T cells were cultured under Th1 or Th17 polarizing conditions. On day 4, intracellular cytokine staining and surface staining for CD11a (tinted histogram, isotype control; black line, anti-CD11a expression) were performed. Shown are representatives of two independent experiments. (C and D) Starting from day 5 after induction of EAE in wild-type and  $\alpha 4^{-/-}$  mice, control rat IgG or antibodies to CD11a were administered i.p. every other day until the development of clinical signs of disease. (C) Means of clinical scores  $\pm$  SEM are depicted according to the classical EAE score ( $n = 6$ ). The rat IgG control-treated and anti-CD11a-treated  $\alpha 4^{-/-}$  groups were compared with two-way ANOVA and Bonferroni's post-testing. (D) Treatment effect of anti-CD11a in  $\alpha 4^{-/-}$  mice according to the ataxia score (mean  $\pm$  SEM,  $n = 4$ ). The two groups were compared with two-way ANOVA and Bonferroni's post-testing. (E and F) Absolute numbers of brain-infiltrating T cells isolated at the peak of disease from wild-type (E) and  $\alpha 4^{-/-}$  mice (F) without or with anti-CD11a treatment (means  $\pm$  SD of absolute CD4 $^{+}$  T cell numbers,  $n = 6$ , Student's *t* test).

integrins in wild-type C57BL/6 mice fails to abolish MOG<sub>35–55</sub>-induced EAE (Kerfoot et al., 2006; not depicted), suggesting that different subsets of encephalitogenic T cells are differentially dependent on  $\alpha 4$  integrin expression to induce CNS

inflammation. However, it has been difficult to dissect the relative contribution of Th1 versus Th17 cells to tissue damage because both species are induced upon immunization with MOG<sub>35–55</sub>/CFA, and because the role of double-producing IFN- $\gamma$  $^{+}$ /IL-17 $^{+}$  CD4 $^{+}$  T cells, as well as the plasticity of pre-committed effector Th17 cells that might modify their cytokine profile toward production of IFN- $\gamma$  during an immune reaction, is incompletely understood in vivo (Lee et al., 2009; Hirota et al., 2011). Yet, in vitro differentiated Th1 and Th17 cells have exquisitely distinct gene expression profiles. Apart from strict differences in the lineage defining genes like *Tbx21*, *Stat1*, *Stat4*, and *Ifng* and *Rorc*, *Rora*, *Stat3*, *Il17*, *Il22*, and *Il23r* for Th1 and Th17 cells, respectively (Korn et al., 2009), we found a sustained down-regulation of  $\alpha 4$  integrin in Th17 cells, whereas Th1 cells kept high expression of  $\alpha 4$  integrins. We have formally tested the hypothesis of differential usage of  $\alpha 4$  by Th1 versus Th17 cells in EAE by analyzing T cell conditional  $\alpha 4^{-/-}$  mice. T cell conditional  $\alpha 4^{-/-}$  mice were not protected from actively induced EAE and developed an atypical disease with predominant brain stem and forebrain infiltrates of IL-23R $^{-}$ , IL-22 $^{-}$ , and CCR6-expressing CD4 $^{+}$  T cells, whereas the spinal cord was relatively spared. In contrast, wild-type littermates always showed classical EAE with predominant spinal cord infiltrates. Together, the clinical and immunopathological phenotypes of actively immunized  $\alpha 4^{-/-}$  mice were reminiscent of adoptive transfer EAE induced with in vitro differentiated Th17 cells. In contrast, Th1-induced EAE consistently resulted in spinal cord syndromes.

In a series of studies, effector functions of Th1 and Th17 cells have been investigated (Kroenke et al., 2008; O'Connor et al., 2008; Domingues et al., 2010). In the adoptive transfer model of Kroenke et al. (2008), clinical signs of Th1- and Th17-induced EAE are indistinguishable, whereas inflammatory infiltrates are dominated by macrophages or neutrophils under conditions of Th1 or Th17 cell transfer, respectively. However, Th1 and Th17 responses have also been associated with different topologies of infiltration within the CNS during EAE (Stromnes et al., 2008). C3H.SW (H-2b) mice develop classical EAE with ascending paralysis, whereas C3HeB/FeJ (H-2k) mice get ataxic disease upon immunization with full-length MOG protein. Here, the ratio of Th17 versus Th1 cells in the autoantigen-specific immune response that develops in the secondary lymphoid organs determines the site of infiltration in the CNS. When the Th17/Th1 ratio exceeds 1, brain infiltration with atypical signs of disease occurs. When the immune response is dominated by Th1 cells, the animals develop classical EAE with spinal cord infiltrates (Stromnes et al., 2008). We propose that differential integrin equipment might promote the targeting of T helper effector subsets into distinct niches of the CNS. Encephalitogenic T cells of the Th17 phenotype are recruited to periventricular areas of the CNS in an  $\alpha 4$  integrin-independent manner, and it is possible that the entry route into the CNS via the cerebrospinal fluid space (Brown and Sawchenko, 2007; Kivisäkk et al., 2009b) is mainly used by T cells that have been committed to the Th17 phenotype. When expression of  $\alpha 4$  integrin is not mandatory for Th17 cells to enter the CNS, which are the molecular cues that guide Th17 cells into the CNS? It has been proposed that Th17

cells are capable of using the uninflamed choroid plexus epithelium as a port of entry in a CCR6/CCL20-dependent manner (Reboldi et al., 2009), although conflicting results exist on the overall susceptibility of CCR6-deficient mice during an inflammatory reaction and particularly during EAE (Elhofy et al., 2009; Villares et al., 2009). Indeed, the amounts of CCR6 and IL-23R expression that are associated with the Th17 phenotype (Petermann et al., 2010) were higher in CD4<sup>+</sup> T cells recovered from the cerebrum of  $\alpha 4^{-/-}$  animals than in wild-type controls. Chemokine receptors are required to activate integrins for cells to adhere to and diapedese through endothelial and epithelial barriers. Besides CCR6, Th17 cells express high amounts of LFA-1. Notably, antibody blockade of LFA-1 abrogated EAE in T cell conditional  $\alpha 4^{-/-}$  mice. Therefore, we provide *in vivo* evidence that encephalitogenic T cells that acquire features of the Th17 lineage in the peripheral immune compartment are capable of infiltrating the brain stem and forebrain in a VLA-4-independent but LFA-1-dependent manner. In contrast to  $\alpha 4^{-/-}$  mice, wild-type mice could not be protected from EAE by treatment with anti-CD11a antibodies. This is consistent with previous studies on anti-LFA-1 treatment in adoptive transfer EAE that was shown to either be inefficient or disease promoting (Cannella et al., 1993; Welsh et al., 1993). Based on our observations in the present study, we propose that blockade of LFA-1 is particularly inefficient to prevent Th1 cells from entering the CNS. Active induction of EAE in LFA-1 KO mice (*Cd11a<sup>-/-</sup>*) has yielded conflicting results (Gültner et al., 2010; Hu et al., 2010), which might be attributed to the fact that LFA-1 is not only involved in diapedesis of T cells across endothelial barriers but also has a prominent role as a costimulatory molecule. Yet, the interaction of LFA-1 with ICAM-1 has been previously identified to support the trafficking of Th17 cells into lung tissue and skin in a systemic sclerosis model (Yoshizaki et al., 2010) and the transmigration of Th17 cells across a confluent layer of primary human endothelial cells *in vitro* (Kebir et al., 2009).

Apart from effector cell intrinsic properties, the tissue responsiveness to certain cytokines has also been implicated in the disease phenotype. When CNS tissue cannot sense IFN- $\gamma$ , as for example in IFN- $\gamma$  receptor-deficient animals, the spinal cord appears to be relatively spared from immunopathology, whereas infiltrates occur in the brain stem and cerebellum, suggesting that local properties of the target tissue contribute to determining the susceptibility to Th1 versus Th17 responses and the extent of immunopathology (Wensky et al., 2005; Lees et al., 2008). It is possible that additional tissue-intrinsic properties, like for example a distinct adhesion molecule expression pattern on endothelial and epithelial surfaces in the CNS (Steffen et al., 1996), the laminin composition of the basement membrane (Wu et al., 2009), the local endothelium associated chemokine milieu (Cruz-Orengo et al., 2011), or the structure and function of endothelial cell junctions (Schulte et al., 2011), contribute not only to the general response of a given organ to inflammation but also determine the topography and dynamics of inflammatory lesions (Engelhardt and Sorokin, 2009).

On the side of the invading immune cells, our data suggest that encephalitogenic T cells are able to enter the CNS in the

absence of  $\alpha 4$  integrins. When T cells lack expression of  $\alpha 4$  integrins, they can still migrate to supraspinal parts of the CNS when they have been committed to the Th17 lineage. In contrast, Th1 cells express  $\alpha 4$  integrins and  $\alpha 4$  integrin expression is necessary and sufficient for Th1 cells to enter into the spinal cord parenchyma. Thus, analysis of the requirement for specific integrins on the surface of distinct T helper cell subsets might be a means to increase our understanding of the topographical distribution of lesions in the CNS during an autoimmune response. Indeed, the clinical phenotype and the type of physical handicap in EAE and MS are profoundly dependent on whether a given inflammatory lesion occurs in the spinal cord or the brain. Besides the hypothesis of differential antigen presentation in different parts of the CNS (Bettelli et al., 2006a; Krishnamoorthy et al., 2006), in this paper we provide evidence that not only the specificity but also the phenotype of T helper effector cells that comes along with a specific integrin equipment is an important determinant of lesion localization within the CNS. Because anti-VLA-4 (natalizumab) treatment has proven a very efficient therapy for human multiple sclerosis and largely abrogates T cell trafficking to the CNS (del Pilar Martin et al., 2008; Kivisäkk et al., 2009a; Stüve et al., 2009), we propose that human encephalitogenic T cells might more resemble Th1 than Th17 cells in the mouse model of EAE. Conversely, MS patients who do not respond to natalizumab often have very active and atypical disease which might be more akin to a Th17 disease (Berger, 2008; Rinaldi et al., 2009). Notably, breakthrough disease in natalizumab-treated patients with opticospinal MS or neuro-myelitis optica has been reported to heavily affect supraspinal parts of the CNS that are not usually targeted by the immune response in this disease entity in the first place (Barnett et al., 2011).

In conclusion, Th1 and Th17 cells depend on  $\alpha 4$  and  $\beta 2$  integrins in a differential manner when migrating into the CNS. Thus, a more profound understanding of the functional phenotype of distinct effector T helper cell subsets *in vivo* might help to approach the enigma of random topographical localization of lesions in MS. Further studies are required to define the interplay between the functional phenotype of T cells and properties of the host tissue that eventually determines the efficacy of immunosurveillance in health and the topography of lesion development in disease.

## MATERIALS AND METHODS

**Animals and induction of EAE.** 2D2 MOG<sub>35-55</sub> TCR-specific transgenic mice (Bettelli et al., 2003), *Foxp3gfp*.KI mice (Bettelli et al., 2006b; Korn et al., 2007), and  $\alpha 4^{fl/fl}$  mice (Scott et al., 2003) have been described previously. CD4 Cre mice, *Ifng<sup>-/-</sup>* mice, *Rag1<sup>-/-</sup>* mice, and wild-type C57BL/6 mice were obtained from The Jackson Laboratory. All mouse strains were on pure C57BL/6 background.

EAE was induced by subcutaneous immunization with 100  $\mu$ g of an emulsion of MOG<sub>35-55</sub> peptide (MEVGWYRSPFSRVVHLVRNGK) and 250  $\mu$ g *Mycobacterium tuberculosis* H37Ra (BD) in Freund's adjuvant oil (CFA) plus i.p. injection of 200 ng pertussis toxin (Fluka) on days 0 and 2. For *in vivo* blockade of CD11a, MOG<sub>35-55</sub>-immunized mice were treated with i.p. injections of anti-CD11a (M17/4; Bio-XCell) or isotype control starting on day 5 (200  $\mu$ g) followed by i.p. injections of 100  $\mu$ g on days 7, 9, and 11 until the development of first signs of disease.

For adoptive transfer experiments, naive FACS-sorted T cells (CD4<sup>+</sup> CD44<sup>-</sup> Foxp3<sup>-</sup> or CD4<sup>+</sup>CD44<sup>+</sup>CD25<sup>-</sup>) from 2D2 × *Foxp3gfp*.KI or 2D2 × *Ifng*<sup>-/-</sup> mice were differentiated in vitro in Th1 or Th17 cells. Differentiation status was checked on day 4 by intracellular cytokine staining and 2 × 10<sup>6</sup> cytokine-positive T cells were injected i.v. into *Rag1*<sup>-/-</sup> recipient mice. Before transfer, Th1 and Th17 cells were incubated with blocking antibodies to α4 integrin (PS/2; Bio-XCell) or 1 μg/ml isotype control (IgG; R&D Systems). Animals were thereafter treated with i.p. PS/2 or 200-μg isotype control antibody injections every 3 d until the development of clinical disease. Clinical signs of EAE were assessed as reported for classical EAE (Korn et al., 2007). Ataxic EAE was scored, as has recently been suggested (Guyenet et al., 2010), by four clinical sub-tests and categories of ledge walking, hindlimb clasp, gait ataxia, and kyphosis with a maximum of three points in each category resulting in a potential maximum score of 12 points. Animals were kept in a specific pathogen-free facility at the Technical University Munich. All experimental protocols were approved by the standing committee for experimentation with laboratory animals of the Bavarian state authorities (Az 55.2-1-54-2531-88-08) and performed in accordance with the corresponding guidelines.

**T cell differentiation.** Cells were cultured in DME with 10% FCS supplemented with 5 × 10<sup>-5</sup> M β-mercaptoethanol, 1 mM sodium pyruvate, non-essential amino acids, L-glutamine, 100 U/ml penicillin, and 100 μg/ml streptomycin. For in vitro T cell differentiation, CD4<sup>+</sup> T cells were purified from naive splenocytes and lymph node cells with anti-CD4<sup>+</sup> magnetic beads (Miltenyi Biotec). For obtaining naive T cells, CD4<sup>+</sup> T cells were sorted into CD4<sup>+</sup>CD44<sup>-</sup>Foxp3<sup>-</sup> T cells by fluorescence activated cell sorting. T cells were stimulated for 3–5 d with 4 μg/ml of plate-bound antibody to CD3 (145-2C11) and 2 μg/ml antibody to CD28 (PV-1). Recombinant cytokines were added to the differentiation cultures as indicated: 2 ng/ml human TGF-β1, 50 ng/ml mouse IL-6, 25 ng/ml mouse IL-23, 10 ng/ml mouse IL-12, and 10 μg/ml anti-IL-4 (R&D Systems). Where indicated, purified naive 2D2 T cells were differentiated by stimulation with 20 μg/ml MOG<sub>35–55</sub> and irradiated (3,000 rd) syngeneic splenocytes in the presence of the described cytokine cocktails. For restimulation experiments, T cells were rested after primary stimulation in IL-2-containing medium followed by restimulation with 2 μg/ml of plate-bound anti-CD3 and 1 μg/ml of soluble anti-CD28 without recombinant cytokines or in the presence of 5 ng/ml IL-12 or 5 ng/ml IL-23.

**Preparation of CNS mononuclear cells and antibody staining.** Mononuclear cells were isolated from the CNS at the peak of disease. After perfusion through the left cardiac ventricle with cold PBS, subcranial structures were dissected from cerebrum and spinal cords flushed out with PBS by hydrostatic pressure. For separate analysis of brain and spinal cord, spinal cord was dissected from cerebrum and brain stem at the level of the medulla oblongata. CNS tissue was digested with 2.5 mg/ml collagenase D (Roche) and 1 mg/ml DNaseI (Sigma-Aldrich) at 37°C for 45 min. Mononuclear cells were isolated by passing the tissue through a 70-μm cell strainer and Percoll gradient (37 over 70%) centrifugation. Mononuclear cells were removed from the interphase, washed, and resuspended in culture medium for further analysis. Surface staining of T cells was performed with antibodies to CD4 (RM4-5), CD3 (14-2C11), CD11a (M17/4 or 2D7), CD25 (PC61 or 7D4), CD44 (IM7), CD49d (9C10(MR4.4B)), and CCR6 (140706). All antibodies were purchased from BD. The biotinylated antibody to CD154 (MR1) was purchased from eBioscience.

**Intracellular cytokine staining.** Cells were stimulated in culture medium containing 50 ng/ml PMA (Sigma-Aldrich), 1 μg/ml ionomycin (Sigma-Aldrich), and 1 μl/ml monensin (GolgiStop; BD) at 37°C and 5% CO<sub>2</sub> for 4 h. After staining of surface markers, cells were fixed and permeabilized (Cytofix/Cytoperm and Perm/Wash buffer; BD), followed by staining with monoclonal antibodies to mouse IL-17 or IFN-γ (BD) and flow cytometric analysis (CYAN; Beckmann Coulter).

**Quantitative PCR analysis.** For quantitative PCR, RNA was extracted from magnetic bead-purified or flow cytometry-sorted cells ex vivo or after in vitro differentiation using RNeasy columns (QIAGEN). Complementary DNA was transcribed as recommended (Applied Biosystems) and used as template for quantitative PCR. Primer plus probe mixtures were obtained from Applied

Biosystems. The TaqMan analysis was performed on a StepOne system (Applied Biosystems). The gene expression was normalized to the expression of β-actin.

**Antigen-specific proliferative and cytokine responses.** For measurement of proliferation, draining lymph nodes from MOG<sub>35–55</sub>-immunized C57BL/6 wild-type or CD4 Cre × α4<sup>fl/fl</sup> mice were dissected on day 8 after immunization. Single cell suspensions were prepared with a 70-μm strainer and cells were seeded on a 96-well U-bottom plate at a density of 200,000 cells. 48 h after restimulation with MOG<sub>35–55</sub>, cell cultures were pulsed with 1.25 μCi <sup>3</sup>H/well and incubated for 18 h at 37°C. Incorporation of radioactive thymidine was analyzed on a β-scintillation counter (1450 MicroBeta TriLux; PerkinElmer). For CD154 (CD40L) staining, single cell suspensions from draining lymph nodes were restimulated with 30 μg/ml MOG<sub>35–55</sub> for 6 h in the presence of 5 μg/ml brefeldin A during the last 3 h of incubation followed by surface and intracellular staining as described.

**Histology.** Diseased animals were perfused at the peak of disease with cold PBS followed by 4% paraformaldehyde fixation, pH 7.4. Brain and spinal cord tissue were prepared separately, embedded in Tissue-Tek (Sakura) and cryopreserved in liquid nitrogen. Coronal periventricular brain sections and transversal lumbar spinal cord sections were cryotomized at 10-μm thickness (CM3050S; Leica). For light microscopy, sections were stained with hematoxylin and eosin (Sigma-Aldrich). For immunofluorescence staining, sections were fixed with 100% ice cold methanol followed by blocking steps with peroxidase, avidin, and biotin blocking reagents (Vector Laboratories), and with 10% goat serum in PBS-T. Sections were then incubated with rat anti-mouse IL-17 (10 μg/ml PBS-T; clone 400210; R&D Systems) or rat anti-mouse CD3 (10 μg/ml PBS-T; clone KT3; AbD Serotec) overnight at 4°C. After multiple washing steps, sections were incubated with biotin-tagged anti-rat IgG (1:200 in PBS-T; Vector Laboratories), followed by incubation with avidin-biotin complex (Vector Laboratories) and biotinylated tyramide. Antibody binding was detected with Alexa Fluor 488-labeled avidin (1:1,000) for CD3 or Alexa Fluor 555-labeled streptavidin for IL-17 (1:1,000; both Invitrogen). In case of double staining, the sections were blocked with rat IgG (Vector Laboratories) and goat anti-rat IgG Fab fragments (Jackson ImmunoResearch Laboratories) and washed extensively with PBS-T before applying the second monoclonal antibody. The second monoclonal antibody was detected with directly labeled Alexa Fluor 488 anti-rat IgG (1:500; Invitrogen). Nuclear staining was performed with Gold antifade with DAPI (Invitrogen). Images were taken using a microscope (Cell Observer; Carl Zeiss) with a camera (AxioCam MRm; Carl Zeiss).

**Statistical Analysis.** Statistical evaluations of cell frequency measurements and cDNA levels were performed with the unpaired Student's *t* test. EAE scores and ataxia scores were evaluated with two-way ANOVA and Bonferroni's post-testing. Two-tailed *p*-values <0.05 were considered significant.

**Online supplemental material.** Video 1 shows atypical EAE in Th17-transferred and anti-α4 antibody-treated Rag1-deficient mice. Online supplemental material is available at <http://www.jem.org/cgi/content/full/jem.20110434/DC1>.

We would like to thank S. Woeste for skillful technical assistance.

V. Rothhammer receives funding from the Gemeinnützige Hertie-Stiftung (1.01.1/10/010). T. Korn is recipient of a Heisenberg grant and other grants from the Deutsche Forschungsgemeinschaft (KO 2964/3-1, KO 2964/4-1, and KO 2964/5-1).

The authors have no conflicting financial interests.

Submitted: 25 February 2011

Accepted: 26 September 2011

## REFERENCES

Archelos, J.J., S. Jung, M. Mäurer, M. Schmied, H. Lassmann, T. Tamatani, M. Miyasaka, K.V. Toyka, and H.P. Hartung. 1993. Inhibition of experimental autoimmune encephalomyelitis by an antibody to the intercellular adhesion molecule ICAM-1. *Ann. Neurol.* 34:145–154. <http://dx.doi.org/10.1002/ana.410340209>  
 Awasthi, A., L. Riol-Blanco, A. Jäger, T. Korn, C. Pot, G. Galileos, E. Bettelli, V.K. Kuchroo, and M. Oukka. 2009. Cutting edge: IL-23 receptor gp

reporter mice reveal distinct populations of IL-17-producing cells. *J. Immunol.* 182:5904–5908. <http://dx.doi.org/10.4049/jimmunol.0900732>

Barnett, M., J. Prineas, M. Buckland, J. Parratt, and J. Pollard. 2011. Massive astrocyte destruction in neuromyelitis optica despite natalizumab therapy. *Mult. Scler.*

Baron, J.L., J.A. Madri, N.H. Ruddle, G. Hashim, and C.A. Janeway Jr. 1993. Surface expression of  $\alpha 4$  integrin by CD4 T cells is required for their entry into brain parenchyma. *J. Exp. Med.* 177:57–68. <http://dx.doi.org/10.1084/jem.177.1.57>

Bartholomäus, I., N. Kawakami, F. Odoardi, C. Schläger, D. Miljkovic, J.W. Ellwart, W.E. Klinkert, C. Flügel-Koch, T.B. Issekutz, H. Wekerle, and A. Flügel. 2009. Effector T cell interactions with meningeal vascular structures in nascent autoimmune CNS lesions. *Nature*. 462:94–98. <http://dx.doi.org/10.1038/nature08478>

Berger, J.R. 2008. Paradoxically aggressive multiple sclerosis in the face of natalizumab therapy. *Mult. Scler.* 14:708–710. <http://dx.doi.org/10.1177/1352458507087135>

Bettelli, E., M. Pagany, H.L. Weiner, C. Linington, R.A. Sobel, and V.K. Kuchroo. 2003. Myelin oligodendrocyte glycoprotein-specific T cell receptor transgenic mice develop spontaneous autoimmune optic neuritis. *J. Exp. Med.* 197:1073–1081. <http://dx.doi.org/10.1084/jem.20021603>

Bettelli, E., D. Baeten, A. Jäger, R.A. Sobel, and V.K. Kuchroo. 2006a. Myelin oligodendrocyte glycoprotein-specific T and B cells cooperate to induce a Devic-like disease in mice. *J. Clin. Invest.* 116:2393–2402. <http://dx.doi.org/10.1172/JCI28334>

Bettelli, E., Y. Carrier, W. Gao, T. Korn, T.B. Strom, M. Oukka, H.L. Weiner, and V.K. Kuchroo. 2006b. Reciprocal developmental pathways for the generation of pathogenic effector TH17 and regulatory T cells. *Nature*. 441:235–238. <http://dx.doi.org/10.1038/nature04753>

Brown, D.A., and P.E. Sawchenko. 2007. Time course and distribution of inflammatory and neurodegenerative events suggest structural bases for the pathogenesis of experimental autoimmune encephalomyelitis. *J. Comp. Neurol.* 502:236–260. <http://dx.doi.org/10.1002/cne.21307>

Cannella, B., A.H. Cross, and C.S. Raine. 1993. Anti-adhesion molecule therapy in experimental autoimmune encephalomyelitis. *J. Neuroimmunol.* 46:43–55. [http://dx.doi.org/10.1016/0165-5728\(93\)90232-N](http://dx.doi.org/10.1016/0165-5728(93)90232-N)

Cruz-Orengo, L., D.W. Holman, D. Dorsey, L. Zhou, P. Zhang, M. Wright, E.E. McCandless, J.R. Patel, G.D. Luker, D.R. Littman, et al. 2011. CXCR7 influences leukocyte entry into the CNS parenchyma by controlling abluminal CXCL12 abundance during autoimmunity. *J. Exp. Med.* 208:327–339. <http://dx.doi.org/10.1084/jem.20102010>

del Pilar Martin, M., P.D. Cravens, R. Winger, E.M. Frohman, M.K. Racke, T.N. Eagar, S.S. Zamvil, M.S. Weber, B. Hemmer, N.J. Karandikar, et al. 2008. Decrease in the numbers of dendritic cells and CD4+ T cells in cerebral perivascular spaces due to natalizumab. *Arch. Neurol.* 65:1596–1603. <http://dx.doi.org/10.1001/archneur.65.12.noc80051>

Domingues, H.S., M. Mues, H. Lassmann, H. Wekerle, and G. Krishnamoorthy. 2010. Functional and pathogenic differences of Th1 and Th17 cells in experimental autoimmune encephalomyelitis. *PLoS ONE*. 5:e15531. <http://dx.doi.org/10.1371/journal.pone.0015531>

Durelli, L., L. Conti, M. Clerico, D. Boselli, G. Contessa, P. Ripellino, B. Ferrero, P. Eid, and F. Novelli. 2009. T-helper 17 cells expand in multiple sclerosis and are inhibited by interferon-beta. *Ann. Neurol.* 65:499–509. <http://dx.doi.org/10.1002/ana.21652>

Elhofy, A., R.W. Depaolo, S.A. Lira, N.W. Lukacs, and W.J. Karpus. 2009. Mice deficient for CCR6 fail to control chronic experimental autoimmune encephalomyelitis. *J. Neuroimmunol.* 213:91–99. <http://dx.doi.org/10.1016/j.jneuroim.2009.05.011>

Engelhardt, B., and L. Sorokin. 2009. The blood-brain and the blood-cerebrospinal fluid barriers: function and dysfunction. *Semin. Immunopathol.* 31:497–511. <http://dx.doi.org/10.1007/s00281-009-0177-0>

Gültner, S., T. Kuhlmann, A. Hesse, J.P. Weber, C. Riemer, M. Baier, and A. Hutloff. 2010. Reduced Treg frequency in LFA-1-deficient mice allows enhanced T effector differentiation and pathology in EAE. *Eur. J. Immunol.* 40:3403–3412. <http://dx.doi.org/10.1002/eji.201040576>

Guyenet, S.J., S.A. Furrer, V.M. Damian, T.D. Baughan, A.R. La Spada, and G.A. Garden. 2010. A simple composite phenotype scoring system for evaluating mouse models of cerebellar ataxia. *J. Vis. Exp.* pii:1787.

Gyölvészi, G., S. Haak, and B. Becher. 2009. IL-23-driven encephalotropism and Th17 polarization during CNS-inflammation in vivo. *Eur. J. Immunol.* 39:1864–1869. <http://dx.doi.org/10.1002/eji.200939305>

Hirota, K., H. Yoshitomi, M. Hashimoto, S. Maeda, S. Teradaira, N. Sugimoto, T. Yamaguchi, T. Nomura, H. Ito, T. Nakamura, et al. 2007. Preferential recruitment of CCR6-expressing Th17 cells to inflamed joints via CCL20 in rheumatoid arthritis and its animal model. *J. Exp. Med.* 204:2803–2812. <http://dx.doi.org/10.1084/jem.20071397>

Hirota, K., J.H. Duarte, M. Veldhoen, E. Hornsby, Y. Li, D.J. Cua, H. Ahlfors, C. Wilhelm, M. Tolaini, U. Menzel, et al. 2011. Fate mapping of IL-17-producing T cells in inflammatory responses. *Nat. Immunol.* 12:255–263. <http://dx.doi.org/10.1038/ni.1993>

Hu, X., J.E. Wohler, K.J. Dugger, and S.R. Barnum. 2010. beta2-integrins in demyelinating disease: not adhering to the paradigm. *J. Leukoc. Biol.* 87:397–403. <http://dx.doi.org/10.1189/jlb.1009654>

Jäger, A., V. Dardalhon, R.A. Sobel, E. Bettelli, and V.K. Kuchroo. 2009. Th1, Th17, and Th9 effector cells induce experimental autoimmune encephalomyelitis with different pathological phenotypes. *J. Immunol.* 183:7169–7177. <http://dx.doi.org/10.4049/jimmunol.0901906>

Keib, H., I. Ifergan, J.I. Alvarez, M. Bernard, J. Poirier, N. Arbour, P. Duquette, and A. Prat. 2009. Preferential recruitment of interferon-gamma-expressing TH17 cells in multiple sclerosis. *Ann. Neurol.* 66:390–402. <http://dx.doi.org/10.1002/ana.21748>

Kerfoot, S.M., M.U. Norman, B.M. Lapointe, C.S. Bonder, L. Zbytnuik, and P. Kubes. 2006. Reevaluation of P-selectin and alpha 4 integrin as targets for the treatment of experimental autoimmune encephalomyelitis. *J. Immunol.* 176:6225–6234.

Kivisäkk, P., B.C. Healy, V. Viglietta, F.J. Quintana, M.A. Hootstein, H.L. Weiner, and S.J. Khouri. 2009a. Natalizumab treatment is associated with peripheral sequestration of proinflammatory T cells. *Neurology*. 72:1922–1930. <http://dx.doi.org/10.1212/WNL.0b013e3181a8266f>

Kivisäkk, P., J. Imitola, S. Rasmussen, W. Elyaman, B. Zhu, R.M. Ransohoff, and S.J. Khouri. 2009b. Localizing central nervous system immune surveillance: meningeal antigen-presenting cells activate T cells during experimental autoimmune encephalomyelitis. *Ann. Neurol.* 65:457–469. <http://dx.doi.org/10.1002/ana.21379>

Korn, T., J. Reddy, W. Gao, E. Bettelli, A. Awasthi, T.R. Petersen, B.T. Bäckström, R.A. Sobel, K.W. Wucherpfennig, T.B. Strom, et al. 2007. Myelin-specific regulatory T cells accumulate in the CNS but fail to control autoimmune inflammation. *Nat. Med.* 13:423–431. <http://dx.doi.org/10.1038/nm1564>

Korn, T., E. Bettelli, M. Oukka, and V.K. Kuchroo. 2009. IL-17 and Th17 Cells. *Annu. Rev. Immunol.* 27:485–517. <http://dx.doi.org/10.1146/annurev.immunol.021908.132710>

Krishnamoorthy, G., H. Lassmann, H. Wekerle, and A. Holz. 2006. Spontaneous opticospatial encephalomyelitis in a double-transgenic mouse model of autoimmune T cell/B cell cooperation. *J. Clin. Invest.* 116:2385–2392. <http://dx.doi.org/10.1172/JCI28330>

Kroenke, M.A., T.J. Carlson, A.V. Andjelkovic, and B.M. Segal. 2008. IL-12- and IL-23-modulated T cells induce distinct types of EAE based on histology, CNS chemokine profile, and response to cytokine inhibition. *J. Exp. Med.* 205:1535–1541. <http://dx.doi.org/10.1084/jem.20080159>

Kuchroo, V.K., C.A. Martin, J.M. Greer, S.T. Ju, R.A. Sobel, and M.E. Dorf. 1993. Cytokines and adhesion molecules contribute to the ability of myelin proteolipid protein-specific T cell clones to mediate experimental allergic encephalomyelitis. *J. Immunol.* 151:4371–4382.

Kuchroo, V.K., M.P. Das, J.A. Brown, A.M. Ranger, S.S. Zamvil, R.A. Sobel, H.L. Weiner, N. Nabavi, and L.H. Glimcher. 1995. B7-1 and B7-2 costimulatory molecules activate differentially the Th1/Th2 developmental pathways: application to autoimmune disease therapy. *Cell*. 80:707–718. [http://dx.doi.org/10.1016/0092-8674\(95\)90349-6](http://dx.doi.org/10.1016/0092-8674(95)90349-6)

Kurschus, F.C., A.L. Croxford, A.P. Heinen, S. Wörtge, D. Ielo, and A. Waisman. 2010. Genetic proof for the transient nature of the Th17 phenotype. *Eur. J. Immunol.* 40:3336–3346. <http://dx.doi.org/10.1002/eji.201040755>

Langrish, C.L., Y. Chen, W.M. Blumenschein, J. Mattson, B. Basham, J.D. Sedgwick, T. McClanahan, R.A. Kastlein, and D.J. Cua. 2005. IL-23 drives a pathogenic T cell population that induces autoimmune inflammation. *J. Exp. Med.* 201:233–240. <http://dx.doi.org/10.1084/jem.20041257>

Laschinger, M., P. Vajkoczy, and B. Engelhardt. 2002. Encephalitogenic T cells use LFA-1 for transendothelial migration but not during capture and initial adhesion strengthening in healthy spinal cord microvessels in vivo. *Eur. J. Immunol.* 32:3598–3606. [http://dx.doi.org/10.1002/1521-4141\(200212\)32:12<3598::AID-IMMU3598>3.0.CO;2-6](http://dx.doi.org/10.1002/1521-4141(200212)32:12<3598::AID-IMMU3598>3.0.CO;2-6)

Lee, Y.K., H. Turner, C.L. Maynard, J.R. Oliver, D. Chen, C.O. Elson, and C.T. Weaver. 2009. Late developmental plasticity in the T helper 17 lineage. *Immunity*. 30:92–107. <http://dx.doi.org/10.1016/j.jimmuni.2008.11.005>

Lees, J.R., P.T. Golumbek, J. Sim, D. Dorsey, and J.H. Russell. 2008. Regional CNS responses to IFN- $\gamma$  determine lesion localization patterns during EAE pathogenesis. *J. Exp. Med.* 205:2633–2642. <http://dx.doi.org/10.1084/jem.20080155>

Lowes, M.A., T. Kikuchi, J. Fuentes-Duculan, I. Cardinale, L.C. Zaba, A.S. Haider, E.P. Bowman, and J.G. Krueger. 2008. Psoriasis vulgaris lesions contain discrete populations of Th1 and Th17 T cells. *J. Invest. Dermatol.* 128:1207–1211. <http://dx.doi.org/10.1038/sj.jid.5701213>

Manel, N., D. Unutmaz, and D.R. Littman. 2008. The differentiation of human T(H)-17 cells requires transforming growth factor-beta and induction of the nuclear receptor ROR $\gamma$ mat. *Nat. Immunol.* 9:641–649. <http://dx.doi.org/10.1038/ni.1610>

Mangan, P.R., L.E. Harrington, D.B. O’Quinn, W.S. Helms, D.C. Bullard, C.O. Elson, R.D. Hatton, S.M. Wahl, T.R. Schoeb, and C.T. Weaver. 2006. Transforming growth factor-beta induces development of the T(H)17 lineage. *Nature*. 441:231–234. <http://dx.doi.org/10.1038/nature04754>

McGeachy, M.J., Y. Chen, C.M. Tato, A. Laurence, B. Joyce-Shaikh, W.M. Blumenschein, T.K. McClanahan, J.J. O’Shea, and D.J. Cua. 2009. The interleukin 23 receptor is essential for the terminal differentiation of interleukin 17-producing effector T helper cells in vivo. *Nat. Immunol.* 10:314–324. <http://dx.doi.org/10.1038/ni.1698>

Mittelbrunn, M., A. Molina, M.M. Escribese, M. Yáñez-Mó, E. Escudero, A. Ursu, R. Tejedor, F. Mampaso, and F. Sánchez-Madrid. 2004. VLA-4 integrin concentrates at the peripheral supramolecular activation complex of the immune synapse and drives T helper 1 responses. *Proc. Natl. Acad. Sci. USA*. 101:11058–11063. <http://dx.doi.org/10.1073/pnas.0307927101>

Murphy, C.A., C.L. Langrish, Y. Chen, W. Blumenschein, T. McClanahan, R.A. Kastlein, J.D. Sedgwick, and D.J. Cua. 2003. Divergent pro- and antiinflammatory roles for IL-23 and IL-12 in joint autoimmune inflammation. *J. Exp. Med.* 198:1951–1957. <http://dx.doi.org/10.1084/jem.20030896>

O’Connor, R.A., C.T. Prendergast, C.A. Sabatos, C.W. Lau, M.D. Leech, D.C. Wraith, and S.M. Anderton. 2008. Cutting edge: Th1 cells facilitate the entry of Th17 cells to the central nervous system during experimental autoimmune encephalomyelitis. *J. Immunol.* 181:3750–3754.

Petermann, F., V. Rothhammer, M.C. Claussen, J.D. Haas, L.R. Blanco, S. Hein, I. Prinz, B. Hemmer, V.K. Kuchroo, M. Oukka, and T. Korn. 2010.  $\gamma\delta$  T cells enhance autoimmunity by restraining regulatory T cell responses via an interleukin-23-dependent mechanism. *Immunity*. 33:351–363. <http://dx.doi.org/10.1016/j.jimmuni.2010.08.013>

Polman, C.H., P.W. O’Connor, E. Havrdova, M. Hutchinson, L. Kappos, D.H. Miller, J.T. Phillips, F.D. Lublin, G. Giovannoni, A. Wajgt, et al; AFFIRM Investigators. 2006. A randomized, placebo-controlled trial of natalizumab for relapsing multiple sclerosis. *N. Engl. J. Med.* 354:899–910. <http://dx.doi.org/10.1056/NEJMoa044397>

Pribila, J.T., A.C. Quale, K.L. Mueller, and Y. Shimizu. 2004. Integrins and T cell-mediated immunity. *Annu. Rev. Immunol.* 22:157–180. <http://dx.doi.org/10.1146/annurev.immunol.22.012703.104649>

Reboldi, A., C. Coisne, D. Baumjohann, F. Benvenuto, D. Bottinelli, S. Lira, A. Uccelli, A. Lanzavecchia, B. Engelhardt, and F. Sallusto. 2009. C-C chemokine receptor 6-regulated entry of TH-17 cells into the CNS through the choroid plexus is required for the initiation of EAE. *Nat. Immunol.* 10:514–523. <http://dx.doi.org/10.1038/ni.1716>

Rinaldi, F., P. Perini, M. Calabrese, L. Rinaldi, and P. Gallo. 2009. Severe relapses after the first infusion of natalizumab in active relapsing-remitting multiple sclerosis. *Mult. Scler.* 15:1359–1362. <http://dx.doi.org/10.1177/1352458509107011>

Schulte, D., V. Küppers, N. Dartsch, A. Broermann, H. Li, A. Zarbock, O. Kamenyeva, F. Kiefer, A. Khandoga, S. Massberg, and D. Vestweber. 2011. Stabilizing the VE-cadherin-catenin complex blocks leukocyte extravasation and vascular permeability. *EMBO J.*

Scott, L.M., G.V. Priestley, and T. Papayannopoulou. 2003. Deletion of alpha4 integrins from adult hematopoietic cells reveals roles in homeostasis, regeneration, and homing. *Mol. Cell. Biol.* 23:9349–9360. <http://dx.doi.org/10.1128/MCB.23.24.9349-9360.2003>

Steffen, B.J., G. Breier, E.C. Butcher, M. Schulz, and B. Engelhardt. 1996. ICAM-1, VCAM-1, and MAdCAM-1 are expressed on choroid plexus epithelium but not endothelium and mediate binding of lymphocytes in vitro. *Am. J. Pathol.* 148:1819–1838.

Steiner, O., C. Coisne, R. Cecchelli, R. Boscacci, U. Deutsch, B. Engelhardt, and R. Lyck. 2010. Differential roles for endothelial ICAM-1, ICAM-2, and VCAM-1 in shear-resistant T cell arrest, polarization, and directed crawling on blood-brain barrier endothelium. *J. Immunol.* 185:4846–4855. <http://dx.doi.org/10.4049/jimmunol.0903732>

Stromnes, I.M., L.M. Cerretti, D. Liggitt, R.A. Harris, and J.M. Goverman. 2008. Differential regulation of central nervous system autoimmunity by T(H)1 and T(H)17 cells. *Nat. Med.* 14:337–342. <http://dx.doi.org/10.1038/nm1715>

Stüve, O., P.D. Cravens, E.M. Frohman, J.T. Phillips, G.M. Remington, G. von Geldern, S. Cepok, M.P. Singh, J.W. Tervaert, M. De Baets, et al. 2009. Immunologic, clinical, and radiologic status 14 months after cessation of natalizumab therapy. *Neurology*. 72:396–401. <http://dx.doi.org/10.1212/01.wnl.0000327341.89587.76>

Vajkoczy, P., M. Laschinger, and B. Engelhardt. 2001. Alpha4-integrin-VCAM-1 binding mediates G protein-independent capture of encephalitogenic T cell blasts to CNS white matter microvessels. *J. Clin. Invest.* 108:557–565.

Villares, R., V. Cadenas, M. Lozano, L. Almonacid, A. Zaballos, C. Martínez-A, and R. Varona. 2009. CCR6 regulates EAE pathogenesis by controlling regulatory CD4+ T-cell recruitment to target tissues. *Eur. J. Immunol.* 39:1671–1681. <http://dx.doi.org/10.1002/eji.200839123>

von Andrian, U.H., and B. Engelhardt. 2003. Alpha4 integrins as therapeutic targets in autoimmune disease. *N. Engl. J. Med.* 348:68–72. <http://dx.doi.org/10.1056/NEJMMe020157>

Wang, Y., H. Kai, F. Chang, K. Shibata, S. Tahara-Hanaoka, S. Honda, A. Shibuya, and K. Shibuya. 2007. A critical role of LFA-1 in the development of Th17 cells and induction of experimental autoimmune encephalomyelitis. *Biochem. Biophys. Res. Commun.* 353:857–862. <http://dx.doi.org/10.1016/j.bbrc.2006.12.104>

Welsh, C.T., J.W. Rose, K.E. Hill, and J.J. Townsend. 1993. Augmentation of adoptively transferred experimental allergic encephalomyelitis by administration of a monoclonal antibody specific for LFA-1 alpha. *J. Neuroimmunol.* 43:161–167. [http://dx.doi.org/10.1016/0165-5728\(93\)90087-F](http://dx.doi.org/10.1016/0165-5728(93)90087-F)

Wensky, A.K., G.C. Furtado, M.C. Marcondes, S. Chen, D. Manfra, S.A. Lira, D. Zagzag, and J.J. Lafaille. 2005. IFN-gamma determines distinct clinical outcomes in autoimmune encephalomyelitis. *J. Immunol.* 174:1416–1423.

Wu, C., F. Ivars, P. Anderson, R. Hallmann, D. Vestweber, P. Nilsson, H. Robenek, K. Tryggvason, J. Song, E. Korpos, et al. 2009. Endothelial basement membrane laminin alpha5 selectively inhibits T lymphocyte extravasation into the brain. *Nat. Med.* 15:519–527. <http://dx.doi.org/10.1038/nm.1957>

Yednock, T.A., C. Cannon, L.C. Fritz, F. Sanchez-Madrid, L. Steinman, and N. Karin. 1992. Prevention of experimental autoimmune encephalomyelitis by antibodies against alpha 4 beta 1 integrin. *Nature*. 356:63–66. <http://dx.doi.org/10.1038/356063a0>

Yoshizaki, A., K. Yanaba, Y. Iwata, K. Komura, A. Ogawa, Y. Akiyama, E. Muroi, T. Hara, F. Ogawa, M. Takenaka, et al. 2010. Cell adhesion molecules regulate fibrotic process via Th1/Th2/Th17 cell balance in a bleomycin-induced scleroderma model. *J. Immunol.* 185:2502–2515. <http://dx.doi.org/10.4049/jimmunol.0901778>

Zheng, Y., D.M. Danilenko, P. Valdez, I. Kasman, J. Eastham-Anderson, J. Wu, and W. Ouyang. 2007. Interleukin-22, a T(H)17 cytokine, mediates IL-23-induced dermal inflammation and acanthosis. *Nature*. 445:648–651. <http://dx.doi.org/10.1038/nature05505>